

## Natural Products

# EBC-232 and 323: A Structural Conundrum Necessitating Unification of Five In Silico Prediction and Elucidation Methods\*\*

Lidia A. Maslovskaya,<sup>[a, b]</sup> Andrei I. Savchenko,<sup>[a]</sup> Elizabeth H. Krenske,<sup>[a]</sup> Sharon Chow,<sup>[a]</sup> Tina Holt,<sup>[c]</sup> Victoria A. Gordon,<sup>[d]</sup> Paul W. Reddell,<sup>[d]</sup> Carly J. Pierce,<sup>[b]</sup> Peter G. Parsons,<sup>[b]</sup> Glen M. Boyle,<sup>[b]</sup> Andrei G. Kutateladze,<sup>[c]</sup> and Craig M. Williams\*<sup>[a]</sup>

**Abstract:** Structurally unique halimanes EBC-232 and EBC-323, isolated from the Australian rainforest plant *Croton insularis*, proved considerably difficult to elucidate. The two diastereomers, which consist an unusual oxo-6,7-spiro ring system fused to a dihydrofuran, were solved by unification

and consultation of five in silico NMR elucidation and prediction methods [i.e., ACDLabs, olefin strain energy (OSE), DP4, DU8+ and TD DFT CD]. Structure elucidation challenges of this nature are prime test case examples for empowering future AI learning in structure elucidation.

## Introduction

Structure determination is a foundational pillar of the discipline of chemistry, but even in modern times this endeavour remains challenging as evidenced by continued reporting of structural mis-assignments,<sup>[1]</sup> especially natural products.<sup>[2]</sup> In view of the spectroscopic resource commitments (e.g., NMR, IR, UV-vis, MS, ECD), available material, and extensive time required to elucidate novel natural products, errors arising from mis-interpretation are mostly understandable.<sup>[3]</sup> Given that interpretation of classical elucidation methods<sup>[4]</sup> are by in large subjective, it is no surprise that development of in silico methods to provide elucidation assistance and insight continues. For example, NMR<sup>[5]</sup> and ECD<sup>[6]</sup> spectra can be predicted from the input of chemical structure, or alternatively software is readily accessible to digest raw spectroscopic data to predict chemical structure (e.g., ACDLabs<sup>[7]</sup>). That said, if many stereoisomers are possible, in silico NMR methods can struggle as standalone entities,<sup>[8]</sup> which often leads to the combination of traditional and in silico elucidation methods being adopted. Al-

though, the latter is not flawless, as chemical synthesis continues to identify errors in elucidation,<sup>[2]</sup> new methods to assist and advance reliable elucidation are constantly being developed (e.g., bridgehead olefin strain energy<sup>[9–12]</sup>).

However, in an age of artificial intelligence (AI), it is no surprise that applications of AI to structure elucidation and synthesis are rapidly growing.<sup>[13]</sup> Computer-assisted structural elucidation (CASE)<sup>[14]</sup> is especially well positioned to play a major role in this regard, but determining the boundaries of in silico elucidation method performance has become critically important.<sup>[15]</sup> Therefore, suitably difficult test case examples are increasingly required.

In the course of undertaking an anti-cancer discovery program investigating the Australian rainforest plant *Croton insularis*,<sup>[8,16]</sup> two unique and closely related spirocyclic halimane diterpenes were identified (i.e., EBC-232 and 323, Scheme 1). The halimane (1) system<sup>[17,18]</sup> is biogenetically derived from geranylgeranyl diphosphate (2), albeit via a rare Me-20 rearranged labdane (3) skeleton.<sup>[18]</sup> The resulting carbocation (i.e., 1) gives rise to three general types of unsaturated halimanes of which EBC-232 and 323 belong to the  $\Delta^{5,10}$ -halimane (4) group.<sup>[17]</sup> Although *C. insularis* had previously yielded the  $\Delta^{5,10}$ -halimane class (e.g., 5 and 6),<sup>[19]</sup> both EBC-232 and 323 were very similar by NMR, identical by mass spectrometry, and prediction methods gave grossly conflicting results (e.g., 7 and 8).

Described herein is the full elucidation of EBC-232 and 323, specifically outlined in stepwise fashion, to purposefully emphasize the vulnerability of reliance on individual methods, and in turn highlights the power of combining not only tangential but aligned in silico NMR methods.

## Results and Discussion

EBC-232 was isolated as a white solid with a molecular ion at  $m/z$  385.1990 [M+Na]<sup>+</sup> (+0.5  $\Delta$ mmu) in positive mode high-resolution electrospray ionization mass spectrometry (HRE-

[a] Dr. L. A. Maslovskaya, Dr. A. I. Savchenko, Prof. E. H. Krenske, Dr. S. Chow, Prof. C. M. Williams  
School of Chemistry and Molecular Biosciences  
University of Queensland, Brisbane, 4072 (Australia)  
E-mail: c.williams3@uq.edu.au

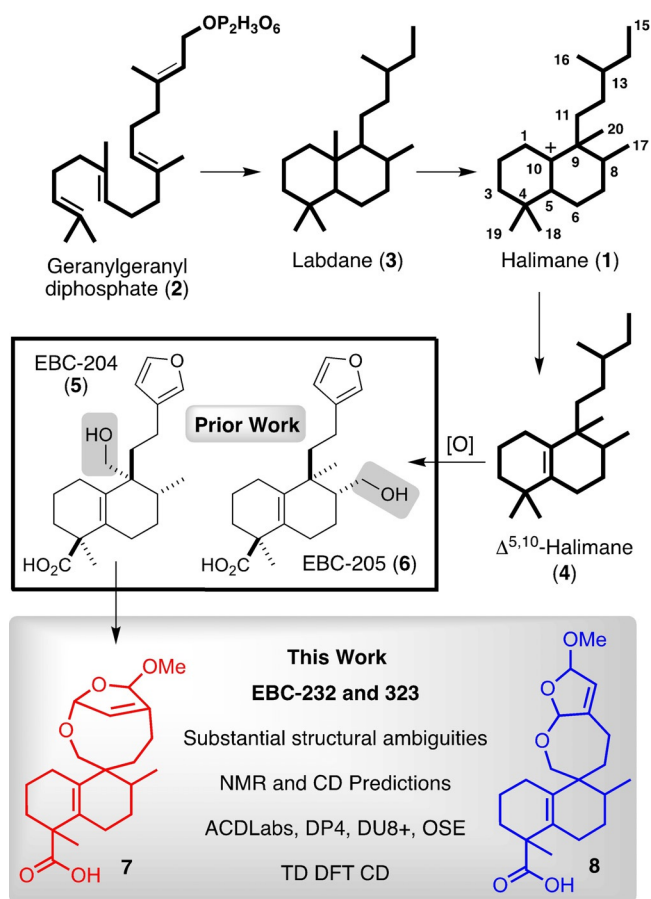
[b] Dr. L. A. Maslovskaya, C. J. Pierce, Prof. P. G. Parsons, Prof. G. M. Boyle  
QIMR Berghofer Medical Research Institute  
PO Royal Brisbane Hospital, Brisbane, 4029 (Australia)

[c] T. Holt, Prof. A. G. Kutateladze  
Department of Chemistry and Biochemistry  
University of Denver, Denver, CO 80208 (USA)

[d] Dr. V. A. Gordon, Dr. P. W. Reddell  
EcoBiotics Limited, PO Box 1, Yungaburra, 4884 Queensland (Australia)

[\*\*] EBC = EcoBiotics Compound.

 Supporting information and the ORCID identification number(s) for the author(s) of this article can be found under:  
 <https://doi.org/10.1002/chem.202001884>



**Scheme 1.** The biogenetic pathway leading to the  $\Delta^{5,10}$ -halimane skeleton (4), including specific known halimane examples EBC-204 (5) and EBC-205 (6), along with proposed flat structures of EBC-232 and 323.

SIMS), corresponding to a molecular formula of  $C_{21}H_{30}NaO_5$  and 7 indices of hydrogen deficiency (IHD). The  $^1H$  NMR spectrum (Table 1) showed one quaternary methyl singlet at 1.25 ppm, one secondary methyl doublet at 0.99 ppm, and one methoxyl at 3.47 ppm. A quaternary oxygenated methylene AB system at 3.38 and 3.85 ppm was clearly present, along with three signals in the range of 5.4–5.7 ppm, which according to their multiplicity indicated different spin systems. The  $^{13}C$  NMR spectrum (Table 1) revealed one carboxylic carbonyl (181.3 ppm), two double bonds and two acetal carbons.

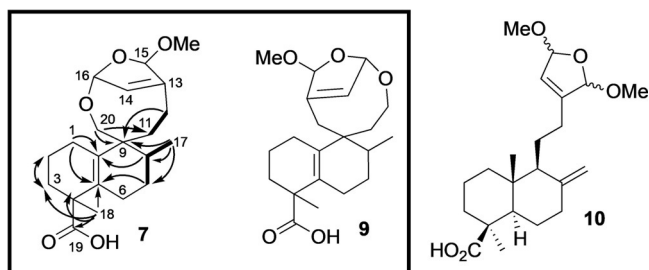
At this point in the elucidation process, ACDLabs NMR Structure Elucidator (version 10.01)<sup>[7]</sup> platform was consulted.<sup>[20]</sup> Raw NMR data,<sup>[21]</sup> along with the molecular formula, were inputted. Two competing top answers were returned, of which both contained the halimane skeleton (i.e., 7 and 9) (Figure 1). This halimane skeleton (specifically the A and B rings) was confirmed by 2D NMR methods. In brief, the connection C7–C8–C17 was made on the basis of well resolved COSY cross peaks for 8-H (2.13 ppm) with Me-17 (0.99 ppm) and 7-H (1.38 and 1.81 ppm), as was the connection C11–C12 on the basis of 12-H (2.37 ppm) correlation with 11-H (1.51 and 1.91 ppm). Heteronuclear multiple bond correlation (HMBC) cross peaks for 17-Me with C9 (44.5 ppm), as well as 20-H (3.38 and 3.85 ppm) with C11 (37.5 ppm), C8 (27.8 ppm) and C9 (44.5 ppm), con-

Table 1. $^1H$ and $^{13}C$ NMR data for EBC-232 and EBC-323 in $CDCl_3$ [ppm].				
Position	$\delta_C^{[a]}$ type	EBC-232 $\delta_H$ mult ( <i>J</i> in Hz, integration) <sup>[b]</sup>	EBC-323 $\delta_C^{[a]}$ type	$\delta_H$ mult ( <i>J</i> in Hz, integration) <sup>[b]</sup>
1a	22.5, $CH_2$	1.69 m (1H)	22.5, $CH_2$	1.71 m (1H)
1b		2.15 m (1H)		2.15 m (1H)
2a,b	19.9, $CH_2$	1.56 m (2H)	19.9, $CH_2$	1.59 m (2H)
3a	36.5, $CH_2$	1.44 ddd (1H, 13.2, 12.5, 3.2)	36.4, $CH_2$	1.44 m (1H)
3b		2.01 m (1H)		2.01 m (1H)
4	46.7, C		46.6, C	
5	129.2, =C		129.6, =C	
6a	24.5, $CH_2$	1.61 m (1H)	24.5, $CH_2$	1.63 m (1H)
6b		1.97 m (1H)		1.82 m (1H)
7a	24.5, $CH_2$	1.38 ddd (1H, 13.4, 6.5, 3.3)	24.4, $CH_2$	1.96 m (2H)
7b		1.81 m (1H)		
8	27.8, CH	2.13 m (1H)	27.8, CH	2.16 m (1H)
9	44.5, C		44.6, C	
10	133.4, =C		133.5, =C	
11a	37.5, $CH_2$	1.51 ddd (1H, 14.1, 13.4, 3.7)	37.7, $CH_2$	1.48 m (1H)
11b		1.91 dddd (1H, 14.0, 4.1, 3.3, 2.3)		1.93 m (1H)
12a	22.2, $CH_2$	2.18 m (1H)	22.1, $CH_2$	2.22 m (1H)
12b		2.37 ddd (1H, 13.1, 4.1, 3.7)		2.41 dt (1H, 13.2, 3.7)
13	145.8, =C		147.8, =C	
14	125.4, =CH	5.73 m (1H)	124.8, =CH	5.74 s (1H)
15	106.8, CH	5.44 q (1H, 0.9)	108.1, CH	5.72 dd (1H, 3.9, 1.4)
16	107.9, CH	5.74 s (1H)	108.5, CH	6.02 dd (1H, 3.9, 1.5)
17	14.2, $CH_3$	0.99 d (3H, 6.8)	14.2, $CH_3$	0.99 d (3H, 6.8)
18	24.1, $CH_3$	1.25 s (3H)	24.1, $CH_3$	1.26 s (3H)
19	181.3, $CO_2H$		179.4, $CO_2H$	
20a	65.0, O- $CH_2$	3.38 dd (1H, 12.7, 2.3)	65.4, O- $CH_2$	3.38 dd (1H, 12.7, 2.5)
20b		3.85 d (1H, 12.7)		3.67 d (1H, 12.7)
21	55.8, O- $CH_3$	3.47 s (3H)	55.1, O- $CH_3$	3.42 s (3H)

[a] 125.77 MHz. [b] 500.13 MHz.

nected C20 (65.0 ppm) to C9 and to fragment C7–C8–C17. HMBC correlations of Me-18 (1.25 ppm) connected C3 (36.5 ppm), C4 (46.7 ppm), C5 (129.2 ppm) and C19 (181.3 ppm) and led to the assignment of a double bond between C5–C10. The cross peaks of 1-H (1.69 ppm) and 8-H (2.13 ppm) with double bond carbons C10 (133.4 ppm) and C5 connected C10 with C1 (22.5 ppm) and C9. The reciprocal interaction of the methylenes at C2 (19.9 ppm), C3 (36.5 ppm), and incorporation of C6 (24.5 ppm), united the carbon skeleton.

Both candidates 7 and 9 also comprised a bicyclic bridgehead alkene,<sup>[11]</sup> which would conceivably originate from furan ring oxidation and *trans*-acetalization with a pendant hydroxyl group. Furan oxidation being a commonly observed biosynthetic transformation has been reported in the labdane series (i.e., 10)<sup>[22]</sup> (Figure 1).



**Figure 1.** Left: Key COSY (bold bonds) and HMBC (curved arrows) correlations for the halimane skeleton (rings A and B) within EBC-232 (**7**) and **9**, the top two proposed candidates from ACDLabs. Right: An example of a labdane with an oxidized furan ring (**10**).

Based on biosynthetic grounds and  $^1\text{H}$  and  $^{13}\text{C}$  NMR shift values of the side chain, candidate **9** could be immediately eliminated. In light of the fact that EBC-204 (**5**), contains a furan ring connected to C12 and with hydroxylation at C20, a spirocycle would be more in-line with that represented by **7** (Figure 1). Furthermore, HMBC correlations revealed supportive connectivity for the bicycle presented in **7**. For example, correlations between 20-H and C16 (107.9 ppm) in the HMBC reinforced acetal functionality at C16. The cross peaks from 15-H to C16 and C21 highlighted mutual interaction with the methoxy group (55.8 ppm) to determine C15 as the second acetal carbon. In addition, 14-H (5.73 ppm) correlated with C12, C13, C15 (106.8 ppm) and C16 (107.9 ppm) seemingly suggesting this bicyclic fragment.

EBC-323, isolated as an unstable white solid, displayed very similar  $^1\text{H}$  and  $^{13}\text{C}$  NMR spectra to those of EBC-232 (Table 1), together with an identical molecular formula ( $\text{C}_{21}\text{H}_{30}\text{O}_5$ ). Therefore, it was logical to presume that EBC-323 was a diastereomer of EBC-232. Indeed, the HMBC cross peaks of Me-17, Me-18 and  $\text{CH}_2$ -20, revealed respective correlations with C3, C4, C5, C7, C8, C9 and C11, which all had similar  $^{13}\text{C}$  chemical shifts (Table 1). However, in this case, although the ACDLabs software again returned two closely ranked candidates, on this occasion the spirocyclic system did not contain a cage bicyclic system seen in **7**, but instead provided **8** as the top ranked answer (Scheme 1).

Given the possibility of two closely related diastereomers, supported by the fact that EBC-323 after 9 months of storage showed isomerization to EBC-232, but not being able to differentiate between the two spirocyclic alternatives, further *in silico* insight was pursued.

Olefin strain (OS) energies were thus calculated according to the method described previously,<sup>[10,12]</sup> with the OPLS 2005<sup>[23]</sup> forcefield. Four likely diastereomers were computed based on stereocentres associated with the halimane/*ent*-halimane<sup>[16,24]</sup> system, NOE data and the acid labile methoxy group (Figure 2). Surprisingly, all structures were calculated to have OS energies in the isolable range.<sup>[10,12]</sup>

Considering that the bridgehead alkenes **11–14** could not be discounted, and that ACDLabs had predicted an alternate structure for EBC-323 (i.e., **8**), theoretical NMR chemical shifts were computed. Accordingly, the DP4 method of Goodman<sup>[25]</sup> was deployed for 12 select isomers (i.e., **11–14** Figure 2, and

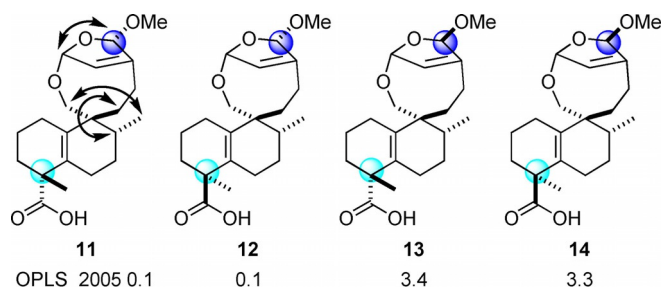


**Figure 2.** Calculated olefin strain energies [ $\text{kcal mol}^{-1}$ ] for bridgehead alkenes **11–14**. Key corroborating NOE correlations shown on **11**.

**15–22** Figure 3) that were considered as possible structures for EBC-232 and EBC-323.

The computed  $^1\text{H}$  and  $^{13}\text{C}$  NMR chemical shifts for **11–22** were then compared to the experimental shifts of EBC-232 and EBC-323 (Tables S1 and S2, see Supporting Information), using various statistical measures of fit for all 12 isomers. However, neither the DP4 calculations, nor the statistical measures of agreement (i.e., mean absolute deviation (MAD), maximum absolute deviation (MaxAD),  $R^2$ ) permitted the structures of EBC-232 and EBC-323 to be unequivocally assigned. That said, the data strongly suggested that two of the bridgehead alkene structures (i.e., **11** and **12**) could be immediately eliminated from further consideration. For example, the  $^{13}\text{C}$  NMR MAD data for **11** and **12** against EBC-232 was about 8 ppm, much higher than the other isomers, which have MAD values in the range of 3–5 ppm. Other measures of fit revealed a similar trend, and similar observations for EBC-323. The calculated chemical shifts for **13** and **14**, albeit in better agreement than **11** and **12**, were a poorer match to experiment than the shifts for the dihydrofurans **15–22**, thus enabling all four bridgehead alkenes to be eliminated from further consideration.

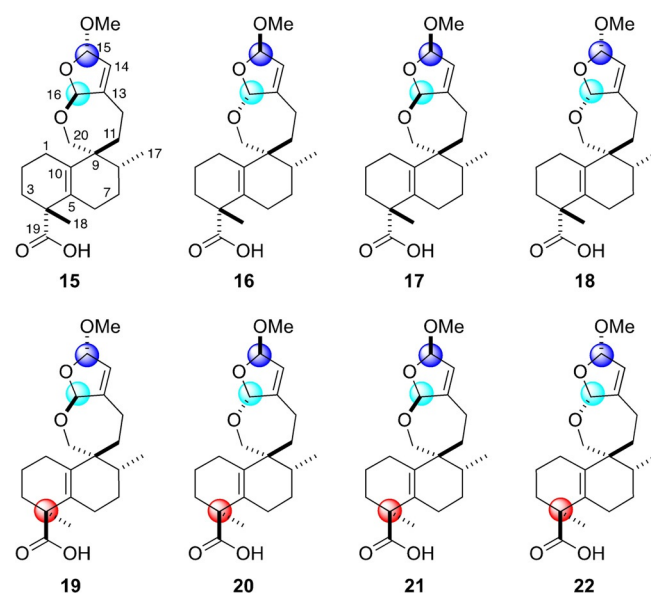


**Figure 3.** Additional isomers considered as possible structures for EBC-232 and EBC-323. For C8 and C9 epimers of **15–22** see Supporting Information.

A broad analysis of the statistical measures revealed two isomers that matched experiment slightly better than the others for both EBC-232 and EBC-323, i.e., **17** and **21**. The overall DP4 probabilities associated with **17** and **21**, for EBC-232, were respectively 7 and 86%, whereas for EBC-323 values of 2 and 40% were obtained, respectively. When the analysis was performed using only  $^1\text{H}$  chemical shifts, the corresponding probabilities for **17** and **21** were 10 and 76% for EBC-232 and 7 and 65% for EBC-323.

Therefore, when all of the above was digested, structure **21** represented a likely candidate for one of the two halimanes. However, given that an assignment could not be unequivocally made based on chemical shifts alone, an alternative approach, DU8+ calculations of NMR coupling constants and chemical shifts,<sup>[5b–g]</sup> were undertaken (Tables S5–18, see Supporting Information).

In the second round of eliminations, **16** and **20** were also discarded based on  $^{13}\text{C}$  chemical shifts alone:  $\text{rmsd}(\delta_{13\text{C}}) > 2.26$  ppm for **16** and  $\text{rmsd}(\delta_{13\text{C}}) > 2.15$  ppm for **20**. The current accuracy of the DU8+ training set of  $> 7100$   $^{13}\text{C}$  chemical shifts, calculated with empirical parametric corrections and a polarizable continuum model (PCM) in chloroform is 1.1 ppm, making a  $\text{rmsd}(\delta_{13\text{C}})$  value of  $> 1.6$  ppm suspicious.

Differentiating between **15**, **17**, and **21** with  $\text{rmsd}$  values ( $\delta_{13\text{C}}$ ) respectively 1.17, 1.23, and 1.06 ppm, was more challenging and required careful analysis of all DU8+ calculated values, that is,  $^1\text{H}$  spin-spin coupling constants and  $^1\text{H}$  and  $^{13}\text{C}$  chemical shifts. As follows from Table 1, eight experimental  $J$  values, twenty-two  $^1\text{H}$  and twenty-two  $^{13}\text{C}$  chemical shift values were available for analysis of EBC-323, while the experimental data for EBC-232 had twenty-one  $J_{\text{HH}}$  values, twenty-three  $^1\text{H}$  and twenty-two  $^{13}\text{C}$  values. The  $^{13}\text{C}$  chemical shift belonging to C19 (carboxylate carbon) was excluded from DU8+ analysis: due to partial dimerization of carboxylic acids in chloroform, the value of this chemical shift is heavily concentration-dependent and therefore unreliable.

Returning to the notion that interconversion of EBC-232 and 323 implies epimerization at an acetal carbon (C15 or C16) leads to two specific dihydrofuran groupings, i.e., **19/21**, **20/22**, **15/17**, **16/18** for epimerization at C15; or **15/18**, **16/17**, **19/22**, **20/21** for epimerization at C16 (Figure 3). Elimination of candidates with poor  $\text{rmsd}(\delta_{13\text{C}})$  values left two potential pairs, **15/17** and **19/21**, and strongly suggested that epimerization at C16 could be ruled out.

Adding to the challenge, all four structures were a rather good match with the experimental data, Table 2. However, it was clear from the experimental data that EBC-323 contained a *trans*-substituted dihydrofuran moiety (i.e.,  $J_{\text{H15-H16}}$  experimental was 3.9 Hz, compared to calculated 4.2 Hz). Whereas for EBC-232 the stereochemistry was assigned as *cis* when considering that the experimental  $J_{\text{H15-H16}}$  was small (calculated 0.8 Hz), and there was a NOE cross-peak between H15-H16. Therefore, the candidate structures for EBC-323 (**15** and **19**—*trans*-dihydrofurans), having fewer experimental constants, all displayed excellent matches to the experimental spin coupling constants (Table 2).

Table 2. DU8+ values for EBC-232 and 323 candidates compared to experimental. <sup>[f]</sup>		
EBC-323	15	19
$\text{rmsd}(J_{\text{HH}})^{[a]}$ (N = 8) <sup>[c]</sup>	0.22 <sup>[d]</sup>	0.20
$\text{rmsd}(\delta_{1\text{H}})^{[b]}$ (N = 22)	0.19 (0.13) <sup>[e]</sup>	0.20 (0.15)
$\text{rmsd}(\delta_{13\text{C}})^{[b]}$ (N = 21)	1.18 (1.15)	0.96 (0.82)
EBC-232	17	21
$\text{rmsd}(J_{\text{HH}})^{[a]}$ (N = 19)	0.21	0.18
$\text{rmsd}(\delta_{1\text{H}})^{[b]}$ (N = 23)	0.23 (0.19)	0.18 (0.10)
$\text{rmsd}(\delta_{13\text{C}})^{[b]}$ (N = 21)	1.22 (1.19)	1.08 (0.95)
Aggregate values for	pair 15/17	pair 19/21
$\text{rmsd}(J_{\text{HH}})^{[a]}$ (N = 27)	0.22	0.19
$\text{rmsd}(\delta_{1\text{H}})^{[b]}$ (N = 45)	0.21 (0.16)	0.19 (0.12)
$\text{rmsd}(\delta_{13\text{C}})^{[b]}$ (N = 42)	1.20 (1.17)	1.03 (0.89)

[a] Hz. [b] ppm. [c] All conformers were weighted according to their DFT energies. [d] RMSDs for  $^1\text{H}$  and  $^{13}\text{C}$  chemical shifts are shown for DU8+ uncorrected data. [e] The values in parenthesis are rmsds with additional linear correction to match the experimental data. [f] Each of the twelve candidate structures **15** through **22** had 10–12 conformers (total of 135) generated and averaged for use in the populations as based on their DFT energies.

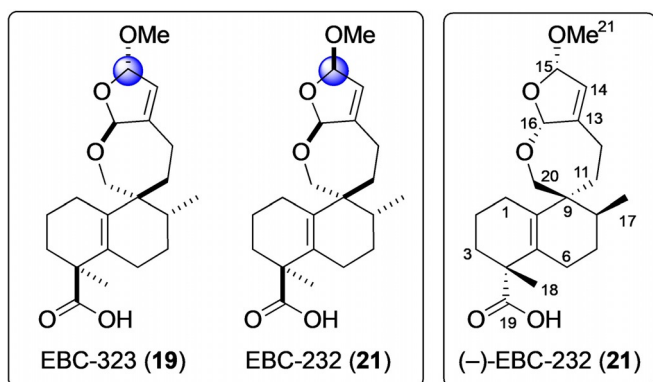
In the case of the *cis*-dihydrofuran grouping (i.e., **17** and **21**) the calculated proton chemical shifts matched slightly better for **21**. A more detailed analysis revealed that this is mostly due to two protons, H3a and H3b. The high field proton H3a (1.44 ppm) in EBC-232 has three nicely defined experimental spin-spin coupling constants (SSCCs) and therefore could not be confused with H3b. The calculated  $^1\text{H}$  chemical shifts demonstrated that the H3 proton which possessed two large (13.3, 12.5 Hz) and one small (3.3 Hz) SSCCs had a higher shift, 1.54 ppm, for structure **21**, but a lower shift, 2.05 ppm, (compared with H3b) for **17**, reinforcing the choice of **21** as the correct diastereomer. Similarly, the experimental chemical shift for its germinal proton (H3b, 2.01 ppm) matches better with the calculated shift in **21**, see Table 3.

Taken in aggregate, all three  $\text{rmsd}$  values pointed to the pair **19/21** as a better match for EBC-323/EBC-232, see Table 2. Therefore, EBC-232 was assigned as **21** and EBC-323 as **19** (Figure 4). DFT calculations predict that **21** is  $\geq 1$  kcal mol<sup>-1</sup> lower in energy than **19**, consistent with the observed conversion of EBC-323 to EBC-232 on storage.

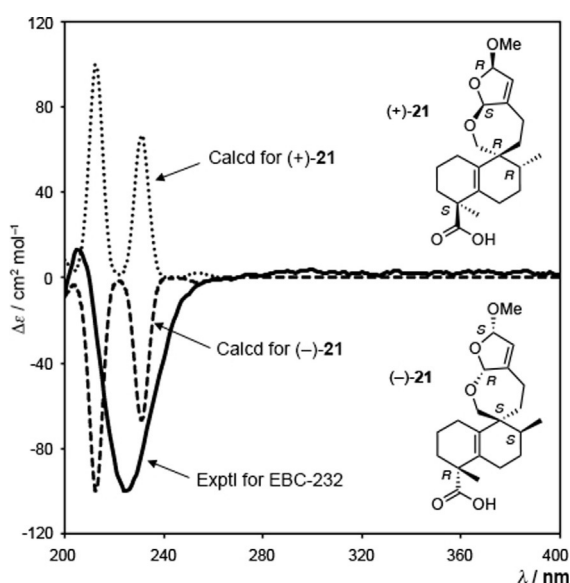
The circular dichroism (CD) spectra were predicted for EBC-232 (**21**), using time-dependent (TD) DFT at the TD-RI-B2PLYP/TZVP level (Figure 4 and Figure 5).<sup>[26]</sup> The computations predicted that, out of the two enantiomers, the *4R*, *8S*, *9S*, *15R*, *16S* enantiomer gave a better match to the experimental ECD spectrum of the isolated material. The isolated sample of EBC-232 had  $[\alpha]_{\text{D}}^{27} - 83.0$  (c 0.08,  $\text{CDCl}_3$ );<sup>[27]</sup> hence the *4R*, *8S*, *9S*,

Table 3. Proton chemical shifts [ppm] for H3a and H3b in EBC-232.

	Exp $\delta_{1\text{H}}$	Calcd for <b>17</b>	Calcd for <b>21</b>
H3a	1.44	2.05	1.54
H3b	2.01	1.61	1.99



**Figure 4.** Elucidated diastereoisomers of EBC-232 (**21**) and EBC-323 (**19**), including absolute stereochemical assignment of EBC-232.



**Figure 5.** Comparison between experimental CD spectrum of EBC-232 and calculated CD spectra of (+)-**21** and (-)-**21**.

15*R*, 16*S* enantiomer is labelled (-)-EBC-232 in Figures 4 and Figure 5.<sup>[27]</sup> Note: the absolute stereochemistry of **19** was not determined.

EBC-232 was tested against cervical (HeLa), colon (HT-29), breast (MCF7), melanoma (MM96L) and leukaemia (K562) cancer cell lines, along with primary neonatal foreskin fibroblast cells (NFF). EBC-323 was only evaluated against MCF7, K562 and NFF due to limited amounts. EBC-232 (**21**) displayed moderate cytotoxic activity towards K562 with an  $IC_{50}$  value of  $16 \pm 7 \mu\text{g mL}^{-1}$ , whereas EBC-323 (**19**) showed stronger activity against the same cell line ( $IC_{50}$  value of  $3 \pm 3 \mu\text{g mL}^{-1}$ ).

## Conclusion

In conclusion, submilligram quantities<sup>[28]</sup> of the unique spirocyclic halimanes EBC-232 (**21**) and 323 (**19**) were isolated from the Australian Rainforest plant *Croton insularis*. The structural assignment of these natural products proved significantly chal-

lenging to elucidate, in that no less than five in silico methods were required (i.e., ACDLabs, OSE, DP4, DU8+, ECD), in tandem, to unravel the northern hemisphere of these diterpenes.

In addition, as structure elucidation continues to head more towards a black box scenario (e.g., applying AI learning to CASE),<sup>[13]</sup> identification of complex chemical structures, that test the performance of modern in silico methods will become more important for CASE evolution.<sup>[29]</sup>

## Experimental Section

Experimental and computational details, along with copies of 1D and 2D NMR spectra are provided in the Supporting Information.

## Acknowledgements

We thank EcoBiotics Ltd., the University of Queensland (UQ), the QIMR Berghofer Medical Research Institute, and the University of Denver for financial support. In addition, we gratefully acknowledge Drs. L. Lambert and G. Pierens from CAI UQ for assistance with NMR measurements. The Australian Research Council for Future Fellowship awards to E.H.K. (FT120100632) and C.M.W. (FT110100851). A.G.K. thanks the US National Science Foundation (CHE1665342) for support. Computational resources were provided by the Australian National Computational Infrastructure through the National Computational Merit Allocation Scheme, and by the UQ Research Computing Centre.

## Conflict of interest

G.M.B. was a recipient of a fellowship co-sponsored by EcoBiotics Ltd. G.M.B., P.G.P. and C.M.W. were recipients of contract research funding from EcoBiotics Ltd.

**Keywords:** Australian rainforest · DP4 · DU8+ · EBC · halimane · in silico

- [1] K. S. Athukorala Arachchige, T. Fahrenhorst-Jones, J. M. Burns, H. A. AL-Fayaad, J. N. Behera, C. N. R. Rao, J. K. Clegg, C. M. Williams, *Chem. Commun.* **2019**, 55, 11751–11753.
- [2] a) K. C. Nicolaou, S. A. Snyder, *Angew. Chem. Int. Ed.* **2005**, 44, 1012–1044; *Angew. Chem.* **2005**, 117, 1036–1069; b) M. E. Maier, *Nat. Prod. Rep.* **2009**, 26, 1105–1124; c) T. L. Suyama, W. H. Gerwick, K. L. McPhail, *Bioorg. Med. Chem.* **2011**, 19, 6675–6701; d) E. E. Podlesny, M. C. Kozlowski, *J. Nat. Prod.* **2012**, 75, 1125–1129; e) For a recent example see, J. M. Fordham, M. N. Grayson, V. K. Aggarwal, *Angew. Chem. Int. Ed.* **2019**, 58, 15268–15272; *Angew. Chem.* **2019**, 131, 15412–15416.
- [3] B. K. Chhetri, S. Lavoie, A. M. Sweeney-Jones, J. Kubanek, *Nat. Prod. Rep.* **2018**, 35, 514–531.
- [4] S. Berger, D. Sicker, *Classics in Spectroscopy: Isolation and Structure Elucidation of Natural Products*, 1st ed., Wiley-VCH, Weinheim, **2009**, pp. 503–512.
- [5] a) M. W. Lodewyk, M. R. Siebert, D. J. Tantillo, *Chem. Rev.* **2012**, 112, 1839–1862; b) A. G. Kutateladze, O. A. Mukhina, *J. Org. Chem.* **2014**, 79, 8397–8406; c) A. G. Kutateladze, O. A. Mukhina, *J. Org. Chem.* **2015**, 80, 5218–5225; d) A. G. Kutateladze, O. A. Mukhina, *J. Org. Chem.* **2015**, 80, 10838–10848; e) A. G. Kutateladze, D. S. Reddy, *J. Org. Chem.* **2017**, 82,

- 3368–3381; f) A. G. Kutateladze, D. M. Kuznetsov, *J. Org. Chem.* **2017**, *82*, 10795–10802; g) A. G. Kutateladze, D. M. Kuznetsov, A. A. Beloglazkina, T. Holt, *J. Org. Chem.* **2018**, *83*, 8341–8352; h) N. Grimblat, A. M. Sarotti, *Chem. Eur. J.* **2016**, *22*, 12246–12261; i) K. Ermanis, K. E. B. Parkes, T. Agback, J. M. Goodman, *Org. Biomol. Chem.* **2017**, *15*, 8998–9007; j) A. Navarro-Vázquez, R. R. Gil, K. Blinov, *J. Nat. Prod.* **2018**, *81*, 203–210; k) J. Wu, P. Lorenzo, S. Zhong, M. Ali, C. P. Butts, E. L. Myers, V. K. Aggarwal, *Nature* **2017**, *547*, 436–440.
- [6] For recent reviews, see: a) S. Superchi, P. Scafato, M. Gorecki, G. Pescitelli, *Curr. Med. Chem.* **2018**, *25*, 287–320; b) G. Pescitelli, T. Bruhn, *Chirality* **2016**, *28*, 466–474.
- [7] A. Moser, M. E. Elyashberg, A. J. Williams, K. A. Blinov, J. C. DiMartino, *J. Cheminf.* **2012**, *4*, 5.
- [8] a) L. A. Maslovskaya, A. I. Savchenko, V. A. Gordon, P. W. Reddell, C. J. Pierce, P. G. Parsons, C. M. Williams, *Eur. J. Org. Chem.* **2016**, 1673–1677; b) L. A. Maslovskaya, A. I. Savchenko, V. A. Gordon, P. W. Reddell, C. J. Pierce, P. G. Parsons, C. M. Williams, *Chem. Eur. J.* **2017**, *23*, 537–540; c) L. A. Maslovskaya, A. I. Savchenko, C. J. Pierce, G. M. Boyle, V. A. Gordon, P. W. Reddell, P. G. Parsons, C. M. Williams, *Chem. Eur. J.* **2019**, *25*, 1525–1534.
- [9] A. I. Savchenko, C. M. Williams, *Eur. J. Org. Chem.* **2013**, 7263–7265.
- [10] a) E. H. Krenske, C. M. Williams, *Angew. Chem. Int. Ed.* **2015**, *54*, 10608–10612; *Angew. Chem.* **2015**, *127*, 10754–10758; b) For application of our method by others, see for example Y. Tang, Y. Xue, G. Du, J. Wang, J. Liu, B. Sun, X.-N. Li, G. Yao, Z. Luo, Y. Zhang, *Angew. Chem. Int. Ed.* **2016**, *55*, 4069–4073; *Angew. Chem.* **2016**, *128*, 4137–4141.
- [11] a) J. Y. W. Mak, R. H. Pouwer, C. M. Williams, *Angew. Chem. Int. Ed.* **2014**, *53*, 13664–13688; *Angew. Chem.* **2014**, *126*, 13882–13906; b) J. Liu, X. Liu, J. Wu, C.-C. Li, *Chem.* **2020**, *6*, 579–615.
- [12] A. G. Kutateladze, E. H. Krenske, C. M. Williams, *Angew. Chem. Int. Ed.* **2019**, *58*, 7107–7112; *Angew. Chem.* **2019**, *131*, 7181–7186.
- [13] a) N. A. B. Gray, *Artif. Intell.* **1984**, *22*, 1–21; b) N. A. B. Gray, *Anal. Chim. Acta* **1988**, *210*, 9–32; c) Z. Hippe, *Artificial Intelligence in Chemistry: Structure Elucidation and Simulation of Organic Reactions*, Elsevier, Warsaw, **1991**; d) E. P. Gajewska, S. Szymkuc, P. Dittwald, M. Startek, O. Popik, J. Mlynarski, B. A. Gryzbowski, *Chem.* **2020**, *6*, 280–293; e) A. Howarth, K. Ermanis, J. M. Goodman, *Chem. Sci.* **2020**, *11*, 4351–4359.
- [14] a) L. Griffiths, *Annu. Rep. NMR Spectrosc.* **2003**, *50*, 217–251; b) R. E. Carhart, D. H. Smith, H. Brown, C. Djerassi, *J. Am. Chem. Soc.* **1975**, *97*, 5755–5762; c) M. Jaspars, *Nat. Prod. Rep.* **1999**, *16*, 241–248; d) A. Williams, *Curr. Opin. Drug Discov. Devel.* **2000**, *3*, 298–305; e) C. Steinbeck, *Curr. Opin. Drug Discov. Devel.* **2001**, *4*, 338–342; f) M. E. Elyashberg, A. J. Williams, G. E. Martin, *Prog. Nucl. Magn. Reson. Spectrosc.* **2008**, *53*, 1–104; g) Y. Liu, J. Saurí, E. Mevers, M. W. Pecuh, H. Hiemstra, J. Clardy, G. E. Martin, R. T. Williamson, *Science* **2017**, *356*, eaam5349; h) D. C. Burns, E. P. Mazzola, W. F. Reynolds, *Nat. Prod. Rep.* **2019**, *36*, 919–933; i) R. Reher, H. W. Kim, C. Zhang, H. H. Mao, M. Wang, L.-F. Nothias, A. M. Caraballo-Rodríguez, E. Glukhov, B. Teke, T. Leao, K. L. Alexander, B. M. Duggan, E. L. Van Everbroeck, P. C. Dorrestein, G. W. Cottrell, W. H. Gerwick, *J. Am. Chem. Soc.* **2020**, *142*, 4114–4120.
- [15] a) J. Bhandari Neupane, R. P. Neupane, Y. Luo, W. Y. Yoshida, R. Sun, P. G. Williams, *Org. Lett.* **2019**, *21*, 8449–8453; b) P. H. Willoughby, M. J. Jansma, T. R. Hoye, *Nat. Protoc.* **2014**, *9*, 643–660.
- [16] a) L. A. Maslovskaya, A. I. Savchenko, V. A. Gordon, P. W. Reddell, C. J. Pierce, P. G. Parsons, C. W. Williams, *Chem. Eur. J.* **2014**, *20*, 14226–14230; b) L. A. Maslovskaya, A. I. Savchenko, E. H. Krenske, C. J. Pierce, V. A. Gordon, P. W. Reddell, P. G. Parsons, C. M. Williams, *Angew. Chem. Int. Ed.* **2014**, *53*, 7006–7009; *Angew. Chem.* **2014**, *126*, 7126–7129; c) L. A. Maslovskaya, A. I. Savchenko, V. A. Gordon, P. W. Reddell, C. J. Pierce, P. G. Parsons, C. M. Williams, *Aust. J. Chem.* **2015**, *68*, 652–659; d) L. A. Maslovskaya, A. I. Savchenko, V. A. Gordon, P. W. Reddell, C. J. Pierce, P. G. Parsons, C. M. Williams, *RSC Adv.* **2016**, *6*, 25110–25113.
- [17] A. M. Roncero, I. E. Tobal, R. F. Moro, D. Díez, I. S. Marcos, *Nat. Prod. Rep.* **2018**, *35*, 955–991.
- [18] a) T. L. Meragelman, D. S. Pedrosa, R. R. Gil, *Biochem. Syst. Ecol.* **2004**, *32*, 45–53; b) J. H. George, M. McArdle, J. E. Baldwin, R. M. Adlington, *Tetrahedron* **2010**, *66*, 6321–6330.
- [19] L. A. Maslovskaya, A. I. Savchenko, V. A. Gordon, P. W. Reddell, C. J. Pierce, G. M. Boyle, P. G. Parsons, C. M. Williams, *Eur. J. Org. Chem.* **2019**, 1058–1060.
- [20] The Williams group have experienced many successful outcomes with the ACDLabs Structure Elucidator program when solving the structures of complex natural products. See for example a) L. Dong, V. A. Gordon, R. L. Grange, J. Johns, P. G. Parsons, A. Porzelle, P. Reddell, H. Schill, C. M. Williams, *J. Am. Chem. Soc.* **2008**, *130*, 15262–15263; b) L. Dong, H. Schill, R. L. Grange, A. Porzelle, J. P. Johns, P. G. Parsons, V. A. Gordon, P. W. Reddell, C. M. Williams, *Chem. Eur. J.* **2009**, *15*, 11307–11318; c) L. A. Maslovskaya, A. I. Savchenko, V. A. Gordon, P. W. Reddell, C. J. Pierce, P. G. Parsons, C. M. Williams, *Org. Lett.* **2011**, *13*, 1032–1035.
- [21] J. B. McAlpine, S.-N. Chen, A. Kutateladze, J. B. MacMillan, G. Appendino, A. Barison, M. A. Beniddir, M. W. Biavatti, S. Bluml, A. Boufridi, M. S. Butler, R. J. Capon, Y. H. Choi, D. Coppage, P. Crews, M. T. Crammins, M. Csete, P. Dewapriya, J. M. Egan, M. J. Garson, G. Genta-Jouve, W. H. Gerwick, H. Gross, M. K. Harper, P. Hermanto, J. M. Hook, L. Hunter, D. Jeanerats, N.-Y. Ji, T. A. Johnson, D. G. I. Kingston, H. Koshino, H.-W. Lee, G. Lewin, J. Li, R. G. Linington, M. Liu, K. L. McPhail, T. F. Molinski, B. S. Moore, J.-W. Nam, R. P. Neupane, M. Niemitz, J.-M. Nuzillard, N. H. Oberlies, F. M. M. Ocampos, G. Pan, R. J. Quinn, D. S. Reddy, J.-H. Renault, J. Rivera-Chávez, W. Robien, C. M. Saunders, T. J. Schmidt, C. Seger, B. Shen, C. Steinbeck, H. Stuppner, S. Sturm, O. Tagliatalata-Scafati, D. J. Tantillo, R. Verpoorte, B.-G. Wang, C. M. Williams, P. G. Williams, J. Wist, J.-M. Yue, C. Zhang, Z. Xu, C. Simmler, D. C. Lankin, J. Bisson, G. F. Pauli, *Nat. Prod. Rep.* **2019**, *36*, 35–107.
- [22] a) C. S. Kim, S. U. Choi, K. R. Lee, *Planta Med.* **2012**, *78*, 485–487; b) This type of oxidation has been replicated in the laboratory, see for example, S. V. Chernov, E. E. Shul'ts, M. M. Shakirov, G. A. Tolstikov, *Russ. J. Org. Chem.* **2006**, *42*, 828–838; and c) S. V. Chernov, E. E. Shul'ts, M. M. Shakirov, G. A. Tolstikov, *Russ. J. Org. Chem.* **2008**, *44*, 67–75.
- [23] J. L. Banks, H. S. Beard, Y. Cao, A. E. Cho, W. Damm, R. Farid, A. K. Felts, T. A. Halgren, D. T. Mainz, J. R. Maple, R. Murphy, D. M. Philipp, M. P. Repasky, L. Y. Zhang, B. J. Berne, R. A. Friesner, E. Gallicchio, R. M. Levy, *J. Comput. Chem.* **2005**, *26*, 1752–1780.
- [24] J. G. Urones, J. de Pascual Teresa, I. Sanchez Marcos, D. Díez Martin, N. Martín Garrido, R. Alfayate Guerra, *Phytochemistry* **1987**, *26*, 1077–1079.
- [25] a) S. G. Smith, J. M. Goodman, *J. Am. Chem. Soc.* **2010**, *132*, 12946–12959; b) DP4 probabilities were calculated with the web applet provided at <http://www.jmg.ch.cam.ac.uk/tools/nmr/DP4/>.
- [26] S. Grimme, *J. Chem. Phys.* **2006**, *124*, 034108.
- [27] Note that (–)-EBC-232 (**21**) has the opposite absolute stereochemistry at C4, C8, and C9 compared with EBC-204 (**5**, Figure 1). The absolute configuration of EBC-204 (**5**), reported previously in ref. [19], was deduced based on a comparison of  $[\alpha]_D$  values to those of related compounds from the literature, and not ECD predictions.
- [28] Innovative NMR equipment and techniques for acquiring improvements in mass-sensitivity have been reported, but potential cost factors have limited wide adoption in some cases, see T. F. Molinski, *Nat. Prod. Rep.* **2010**, *27*, 321–329.
- [29] For recent examples see, a) B. Khatri Chhetri, S. Lavoie, A. M. Sweeney-Jones, N. Mojib, V. Raghavan, K. Gagaring, B. Dale, C. W. McNamara, K. Soapi, C. L. Quave, P. L. Polavarapu, J. Kubanek, *J. Org. Chem.* **2019**, *84*, 8531–8541; b) M. M. Zanardi, M. O. Marcarino, A. M. Sarotti, *Org. Lett.* **2020**, *22*, 52–56.

Manuscript received: April 17, 2020

Revised manuscript received: June 8, 2020

Version of record online: August 30, 2020